Immunohistochemistry and Spatial Density of Müller Cells in the Human Fovea

Rania A. Masri,[1] Ursula Greferath,[2] Erica L. Fletcher,[2] Paul R. Martin,[1] and Ulrike Grünert[1]

[1]The University of Sydney, Faculty of Medicine and Health, Save Sight Institute, Sydney, NSW, Australia
[2]The University of Melbourne, Department of Anatomy and Physiology, Melbourne, VIC, Australia

Correspondence: Ulrike Grünert, Save Sight Institute, University of Sydney, Level 2, Centre Block, 8 Macquarie Street, Sydney, NSW 2000, Australia; ulrike.grunert@sydney.edu.au.

Received: November 19, 2024
Accepted: January 26, 2025
Published: February 18, 2025

Citation: Masri RA, Greferath U, Fletcher EL, Martin PR, Grünert U. Immunohistochemistry and spatial density of Müller cells in the human fovea. *Invest Ophthalmol Vis Sci.* 2025;66(2):46. https://doi.org/10.1167/iovs.66.2.46

Purpose. Previous evidence indicates that molecular properties of foveal Müller cells are different from those in the peripheral retina. Here we aimed to characterize Müller cells in the human fovea (including the foveal floor) with specific focus on their spatial density and immunohistochemistry.

Methods. Human retinas were obtained postmortem from male and female donors with no known eye disease (aged 31–56 years) or after exenteration (one 75-year-old patient with no retinal disease and one 86-year-old patient with reticular pseudodrusen). Vertical sections through the macula were processed for immunofluorescence using antibodies against cellular retinaldehyde binding protein (CRALBP), glutamine synthetase (GS), glial fibrillary acidic protein (GFAP), transient receptor potential vanilloid 4 (TRPV4), excitatory amino acid transporter 4 (EAAT4), calbindin, and RNA-binding protein with multiple splicing. Sections were imaged using high-resolution, multichannel confocal microscopy.

Results. Immunofluorescence for CRALBP and GS was found in Müller cells, including their processes throughout the retina. GFAP expression was found in astrocytes outside the fovea and in some foveal somas. Müller cell nuclei had a peak density of about 35,000 cells/mm^2 at 500 µm eccentricity. Calbindin was coexpressed with CRALBP in up to 96% of Müller cells in the fovea, but at eccentricities beyond about 1.5 mm calbindin was not expressed by Müller cells. Conversely, calbindin expression in cone photoreceptors was absent in foveal but present in peripheral retina.

Conclusions. This study supports the hypothesis that Müller cells in the macula have distinct structural, functional, and immunohistochemical properties compared to their peripheral counterparts.

Keywords: Müller glia, astrocytes, human retina, calbindin, fovea

The fovea is a specialized region in primate retina that serves high visual acuity.[1,4] The center of the fovea (foveola) is characterized by a high cone photoreceptor density, the absence of rod photoreceptors,[5–8] and the lack of retinal vasculature.[9,10] Degeneration of the fovea as in retinal diseases such as advanced age-related macular degeneration (AMD) is a leading cause of irreversible vision loss. Thus understanding the architecture and molecular properties of the fovea is an important scientific goal with high clinical relevance.

The primate retina contains three types of glial cells comprising Müller cells, astrocytes, and microglia that all play critical roles in maintaining normal neural function.[11,12] Müller cells are the most abundant retinal glial cell[13–16] and Müller cell dysfunction has been linked to retinal diseases such as diabetic retinopathy[17] and AMD.[18–20] Moreover, Müller cells have been shown to play a role in neuronal regeneration in zebrafish and mice.[21,22]

In human retina as in other diurnal primates, the morphology of Müller cells varies with the distance from the fovea.[11,16,23–25] Müller cells in peripheral retina (beyond 3 mm eccentricity) resemble their counterparts in other mammals.[26,27] Their cell bodies are situated in the inner nuclear layer, their outer processes end in microvilli which make tight-like junctions with the inner segments of cone and rod photoreceptor to form the outer (external) limiting membrane (OLM), and their endfeet form the inner limiting membrane (ILM). The somas of Müller cells in central retina (0.7 to 3 mm eccentricity) are also located in the inner nuclear layer and their inner processes terminate at the ILM, but their outer processes (which originate in the center of the fovea and contribute to the Henle fiber layer) are elongated and laterally displaced, giving the cells a z-shaped appearance.[16,23]

The foveal floor has been suggested to contain a small population of specialized Müller cells. Polyak[23] (page 203) using light microscopy described these cells as having "dark nuclei with finely granulated chromatin … resembling Müller cell nuclei." A subsequent electron microscopic study described this region as an electron lucent "bowl shaped concavity … containing a large amount of Müller cell processes." The outer processes of these foveal Müller cells envelop the cone nuclei and cone outer processes before terminating at the outer limiting membrane.[28] This region

has been named "Müller cell cone"[29] but is also referred to as the "central foveal bouquet."[30] The latter term is a variation of "bouquet of central cones" coined by Rochon-Duvigneaud in 1907 (cited after Polyak[23]) because it was originally thought to contain cones only. Here we will be using the term *central bouquet* to refer to this region. A more recent EM study found that the inner processes of the Müller cells in the central bouquet do not form endfeet and that their outer processes do not contribute to the Henle fiber layer but extend straight to the outer limiting membrane where they envelope and separate the outer processes of cone photoreceptors.[24]

Evidence from nonhuman primates suggests that in the fovea there are as many Müller cells as cones.[31,32] Similarly, in our previous study of human retina,[33] we estimated that there are between one and two Müller cells per cone in the fovea. However, little is known about the Müller cell density in the foveola of normal human retina.

The cellular retinaldehyde binding protein (CRALBP) is expressed in the retinal pigment epithelium, as well as by Müller cells[34] and is thought to play a role in the regeneration of cone visual pigment and the maintenance of cone function.[35,36] In support of the notion that the foveal floor contains Müller cells, expression of CRALBP and another Müller cell marker, glutamine synthetase (GS) has been found albeit at a reduced level compared to outside of the fovea in human and nonhuman primates.[37–41] In addition, expression of glial fibrillary acidic protein (GFAP) in the foveola has been reported, but these studies differ in the interpretation of the result (astrocytes[38,39] versus Müller cells[16,25]). There is evidence for differences in gene expression between foveal and peripheral (beyond 2.5 mm eccentricity) Müller cells from molecular studies that may point to distinct functions in these two locations.[20,42–47]

The aim of the present study was to compare the immunohistochemical profile of Müller cells in the fovea and peripheral retinal and to quantify their density. We demonstrate that foveal but not peripheral Müller cells of adult human retina express the calcium binding protein calbindin D28K. Conversely, as reported previously[48] we find that cone photoreceptors in the peripheral retina but not in the fovea express calbindin.

Methods

Tissue Collection and Preparation

Information about the donor eyes obtained postmortem is summarized in Table 1. The eyes of six human donors were

Table 1. Postmortem Donor Retinas

ID	Eye	Sex	Age (Years)	Time to Enucleation (H)	Time to Preservation (H)	Fixative	Fixation Time (H)
13587	Right* & Left	F	44	2	4	2% PFA	12
13699	Right* & Left	M	56	2	9	2% PFA	21
14064	Right*	F	44	1	3	2% PFA	13
15415	Left*,†	F	54	3	5	2% PFA	17
15649	Left*	F	36	0.5	8	2% PFA	40
D19-0859	Right & Left	F	31	1	7	2% PFA	16

*These preparations were also used in our previous studies.[19,33,58]
†The eye was placed into CO_2 independent medium for one hour before fixation. Times over one hour are shown to the nearest hour.

Table 2. Antibodies

Antibody Name	Immunogen	Source, Catalogue Number, RRID	Antibody Type	Dilution
CaBP	Recombinant rat calbindin D-28k	Swant, CB38, lot: 5.5, RRID: AB_10000340	Rabbit polyclonal	1:20,000
CaBP	Calbindin D-28k purified from chicken gut	Swant, 300, lot: 07 (F), RRID: AB_10000347	Mouse monoclonal	1:10,000
Cone arrestin (7G6)	Crude extract of macaque light-adapted retina	Gift from Peter MacLeish, Morehouse School of Medicine, Atlanta, GA, RRID: AB_2314215	Mouse monoclonal	1:500
Cellular retinaldehyde binding protein	Recombinant full-length protein corresponding to Human CRALBP	Abcam, AB_15051, lot: F10, 13, RRID: AB_2269474	Mouse monoclonal	1:1,000
Cellular retinaldehyde binding protein (B2)	Human recombinant CRALBP	Thermo Fisher, MA1-813, RRID:AB_2178528	Mouse monoclonal	1:500
EAAT4	21 Amino acid synthetic oligopeptide corresponding to the C-terminus of rat EAAT4	Alpha Diagnostic, EAAT41-A, RRID:AB_1622384	Rabbit polyclonal	1:500
Glial fibrillary acidic protein	GFAP from pig spinal cord	Merck, G3893, RRID: AB_477010	Mouse monoclonal	1:200
Glial fibrillary acidic protein	GFAP (cat, cow, dog, human, mouse, rat, sheep)	DAKO, Z0334, RRID: AB_10013382	Rabbit polyclonal	1:50,000
Glutamine synthetase	Human glutamine synthetase amino acids 1–373	BD Biosciences, 610518; RRID: AB_397880	Mouse monoclonal	1:6,000
TRPV4	Synthetic peptide corresponding to region 742–753 within internal amino acids 720 to 769	Abcam; AB94868, RRID:AB_10675981	Rabbit polyconal	1:200

Investigative Ophthalmology & Visual Science

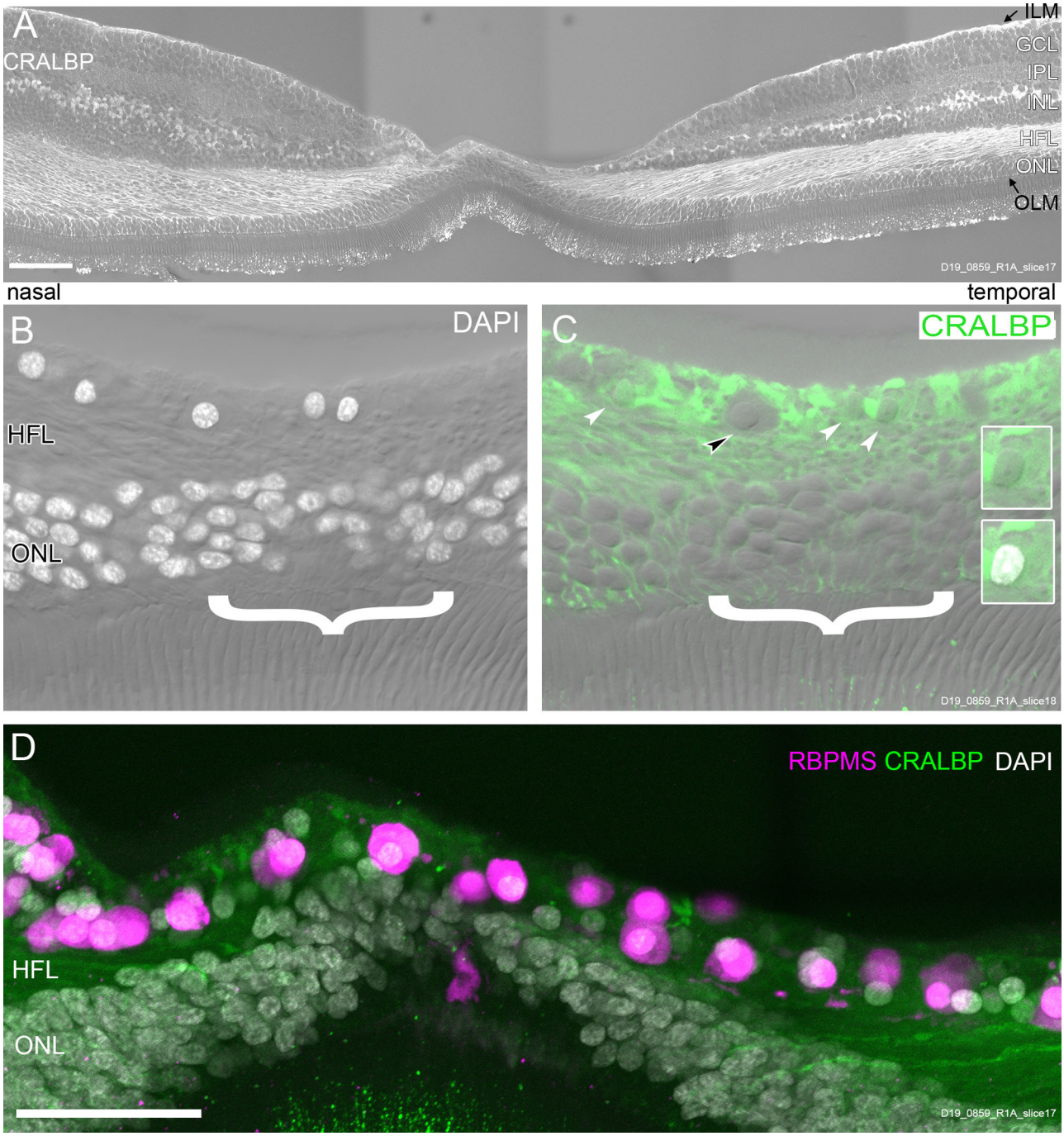

Figure 1. Glia and neurons on the foveal floor. Confocal images of a vertical section through the fovea of a 31-year-old woman (Case no. D19_0859R) processed with antibodies against the Müller cell marker CRALBP and the ganglion cell marker RBPMS. (**A**) Single image from a tiled stack of images showing CRALBP immunofluorescence (*white*) in Müller cells spanning the retina from the OLM to the ILM. DIC optics is used to reveal the retinal layers. (**B**, **C**) This section (adjacent to the one shown in **A**) was processed with DAPI (white) and antibodies against the Müller cell marker CRALBP (*green*). DIC optics reveals the retinal layers. A single image from a stack of images is shown. The *white arrowheads* indicate CRALBP positive Müller cell somas, the *black arrowhead* points to an unlabeled soma. CRALBP immunofluorescence fills the foveal floor and extends to the OLM. The *bracket* indicates the region of the central bouquet. The insets show the soma of the CRALBP-positive cell on the right together with DIC (*top*) and DAPI labeling (*bottom*). (**D**) Maximum-intensity projection of a stack of confocal images showing that the foveal floor comprises RBPMS (*magenta*) positive ganglion cells and CRALBP (*green*) positive Müller cells. The same section as in **A** is shown. GCL, ganglion cell layer; IPL, inner plexiform layer; OPL, outer plexiform layer. *Scale bar* shown in **A**: 100 µm; *scale bar* shown in **D**: 50 µm (applies to **B**–**D**).

Investigative Ophthalmology & Visual Science

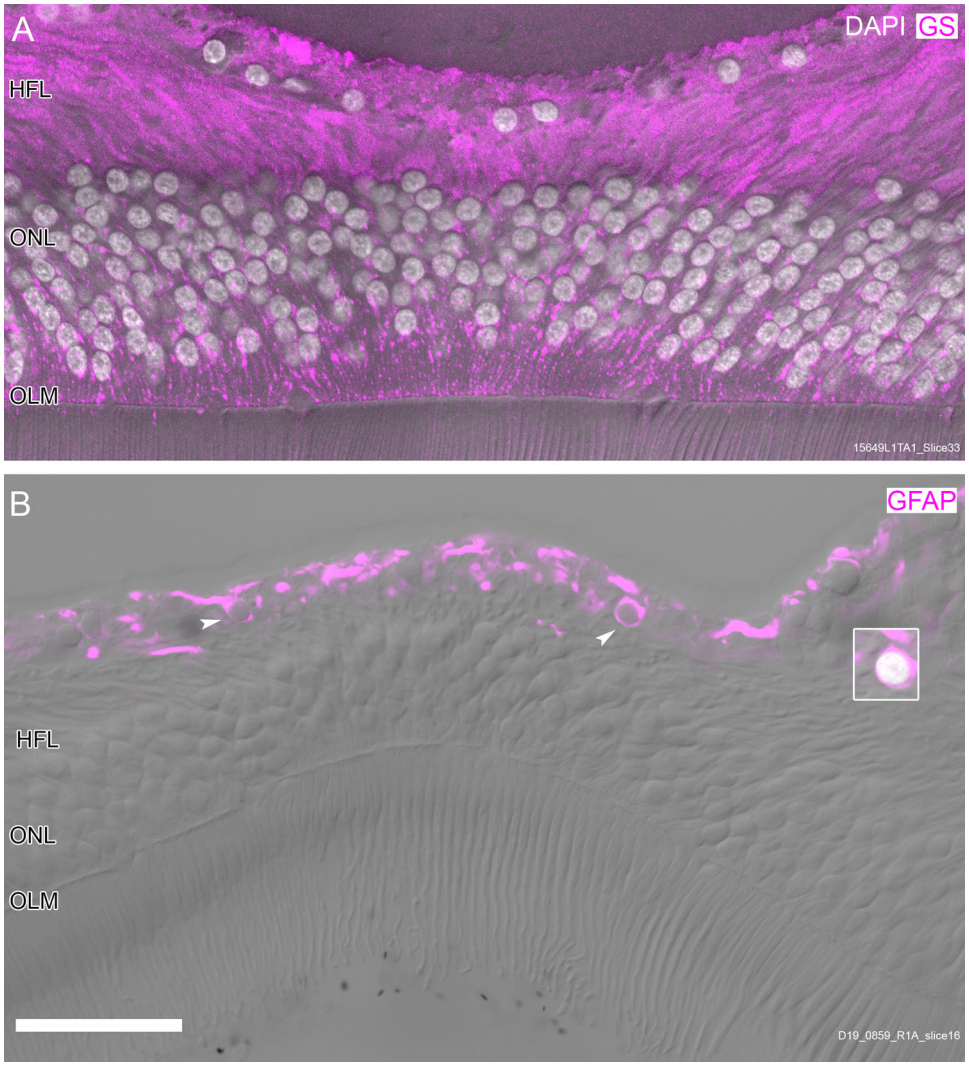

Figure 2. Glial cells on the foveal floor. Confocal images of different vertical sections through the foveal floor of a 36-year-old woman (case no. 15659L, **A**) and a 31-year-old woman (case no. D19_0859R, **B**). (**A**) The section was processed with DAPI (*white*) and antibodies against the Müller cell marker GS (*magenta*). The GS immunofluorescence fills the foveal floor including the HFL and extends to the OLM. (**B**) The section was processed antibodies against the astrocyte marker GFAP (*magenta*). GFAP-positive somas (*white arrowheads*) and their processes are found at the foveal floor. The inset shows the cell indicated on the right together with DAPI staining. DIC optics is used to reveal the retinal layers. *Scale bar*: 50 µm.

obtained from the Lions NSW Eye Bank (Sydney Eye Hospital) and Australian Ocular Biobank with consent and ethical approval from The University of Sydney Human Research Ethics Committee (HREC# 2012/2833). Donor ophthalmologic histories were not available for these eyes but retinas showing obvious pathology such as advanced macular degeneration, distortion of the optic disc (suggesting glaucoma) or intraretinal myelination[49] were excluded from the study.

In addition, we obtained two foveas from two consenting donors whose eyes were exenterated because of a lower lid sebaceous cell carcinoma. One eye from a 86-year-old female donor had widespread reticular pseudodrusen (RPD) throughout the macula (for details see Greferath et al.[50]), and the other eye was from a 75-year-old female donor that, apart from a cataract, had no known eye disease. The approval for these studies was obtained from the Human Ethics Committees of the Royal Victorian Eye and Ear Hospital in Melbourne, Australia (HREC no. 08/0853H/18) and The University of Melbourne (HREC no. 22293).

Retinas from postmortem donors were fixed in the eyecup in 2% paraformaldehyde (PFA) in 0.1M phosphate buffer (PB) less than 10 hours after death. They were rinsed in PB and dissected from the eye cup. Small retinal pieces (3–4 mm in width and 3–5 mm in length) including the fovea were prepared for sectioning along the nasal-temporal axis. Sections were judged to be at the center of the fovea when almost no somas were visible at the foveal floor, the processes in the Henle fiber layer appeared parallel and the nuclear layers did not appear distorted.

The tissue was rinsed in PBS, embedded in 3% low melting temperature Agarose (Sea Plaque Agarose; Lonza, Rockland, ME, USA) in PBS and sectioned at a thickness of 100 µm using a Vibratome (VT 1200; Leica Microsystems, Wetzlar, Germany). In one case (no. 13587L) a piece of retina (4 × 4 mm) centered around the fovea was processed as a flat

Investigative Ophthalmology & Visual Science

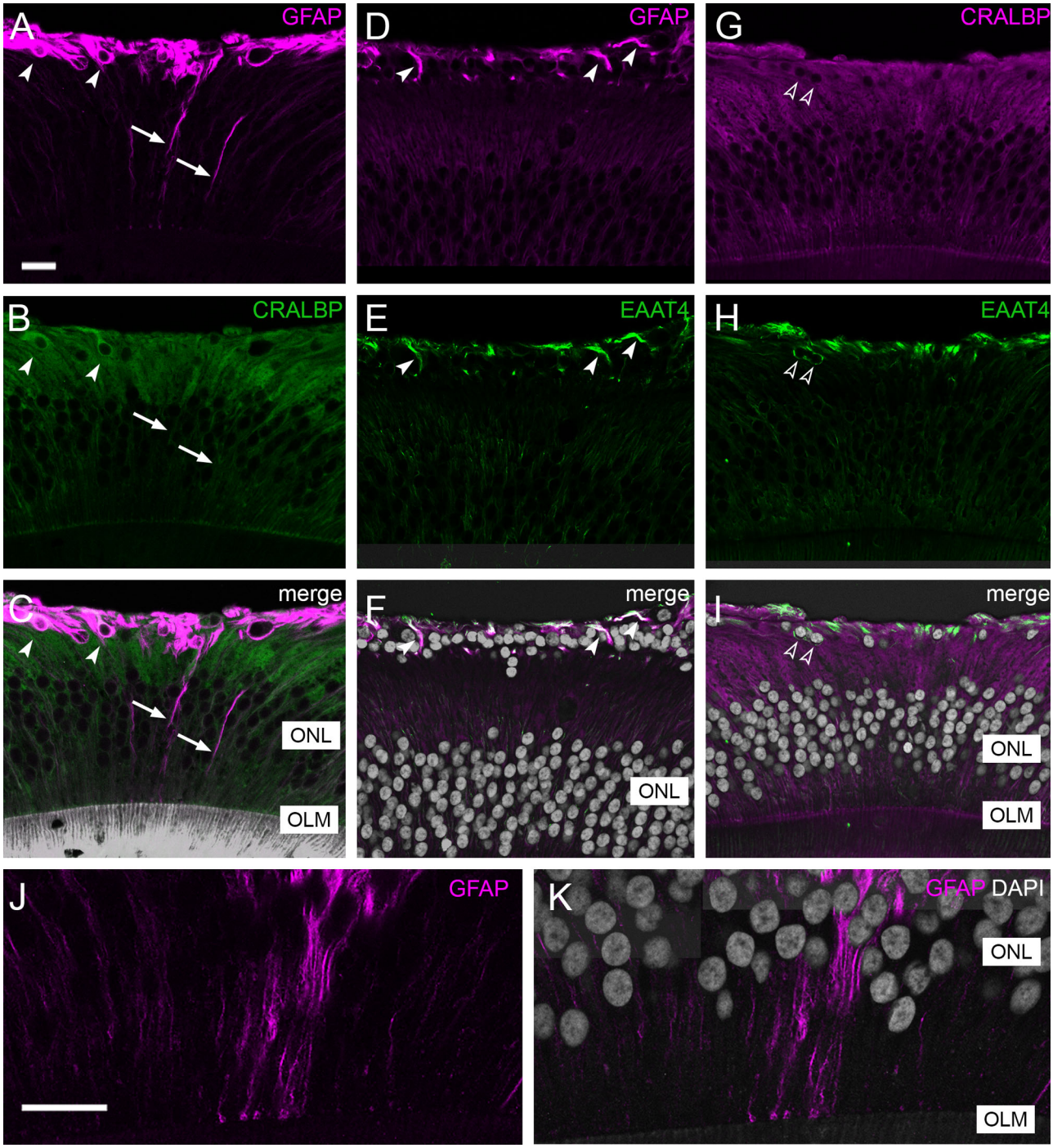

Figure 3. Expression of Müller cell and astrocyte markers on the foveal floor of an 86-year-old woman with RPD. Confocal micrographs of cryostat sections through the foveola. (**A–C**) GFAP (*magenta*) is coexpressed with CRALBP (*green*) in some (*arrowheads*) but not all somas on the foveal floor. Some GFAP expressing processes (*arrows*) extend to the OLM as delineated by labeling for peanut agglutinin expressed by cone inner segments (*white*). These processes do not coexpress CRALBP. (**D–F**) GFAP (*green*) is coexpressed with EAAT4 (*magenta*, *arrowheads*). (**G–I**) EAAT4 positive somas (green) are indicated by *open arrowheads*. These cells do not express CRALBP. (**J**, **K**) High-resolution images of GFAP expressing processes extending to the OLM. ONL, outer nuclear layer. *Scale bar* shown in **A**: 20 µm applies to **A** to **I**; *scale bar* shown in **J**: 20 µm, applies to **J** and **K**.

mount. The human tissue experiments complied with the guidelines of the ARVO Best Practices for Using Human Eye Tissue in Research (Nov2021).

The eyes from the 86-year-old and the 75-year-old donors were exenterated and fixed in 4% PFA in 0.1 M PB (four hours at room temperature) within approximately 20 minutes. The retinal piece containing the fovea was dissected, cryoprotected in graded sucrose solutions (10%, 20%, 30% weight/volume), snap-frozen, and stored at −80°C until use. Sections (14 µm thick) were taken through the middle of the foveola along the horizontal meridian using a cryostat (Reichert Jung) and collected on polylysine

Investigative Ophthalmology & Visual Science

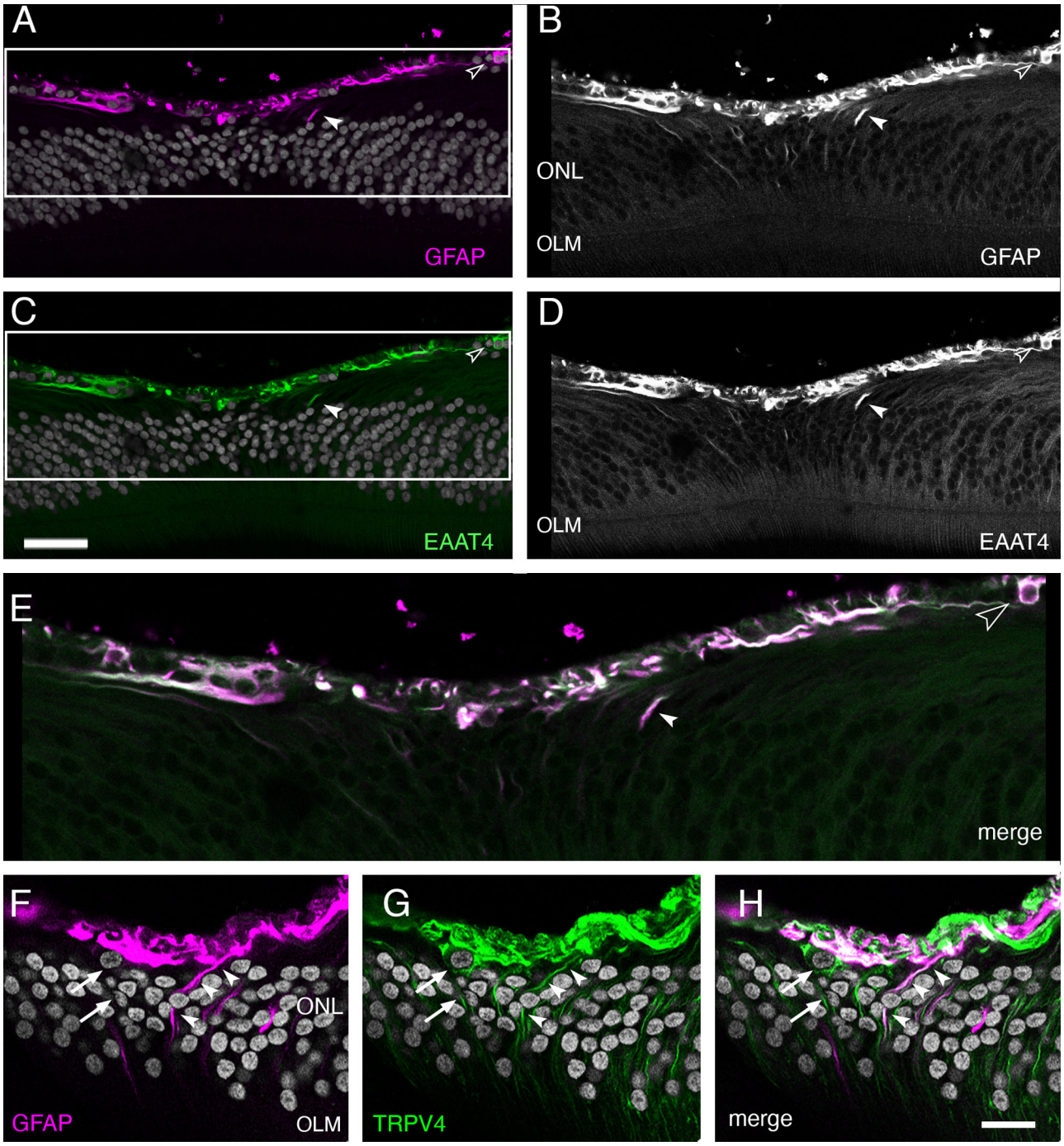

Figure 4. Expression of glial markers on the foveal floor of a 75-year-old woman without retinal disease. Confocal micrographs of cryostat sections through the foveola. (**A–E**) GFAP (*magenta*) is coexpressed with EAAT4 (*green*) in somas (*open arrowheads*) and their processes on the foveal floor, as well as in some processes on extending to the outer limiting membrane (*white arrowheads*). The *boxes* shown in **A** and **C** indicate the region shown in **E**. The images shown in **B** and **D** are the same as in **A** and **C**, respectively, but are showing only the GFAP channel in *black* and *white*. (**F–H**) GFAP (*magenta*) is coexpressed (*white arrowheads*) with TRPV4 (*green*) in some processes. The *arrows* indicate a TRPV4 positive soma and processes that are not double labeled. DAPI-labeled nuclei are shown in *gray*. ONL, outer nuclear layer. *Scale bar* shown in **C**: 50 µm applies to **A–D**; *scale bar* shown in **H**: 20 µm applies to **F–H**.

glass adhesion slides (Thermo Fisher Scientific, Waltham, MA, USA).

Primary Antibodies

The antibodies used in this study are summarized in Table 2. Multiple glial cell markers were used: Antibodies against CRALBP[34] and against GS, the enzyme that converts glutamate to the amino acid glutamine, are known markers of Müller cells.[41,51,52] Antibodies against GFAP[13,14] and excitatory amino acid transporter 4 (EAAT4)[53,54] are established markers for astrocytes but GFAP is also expressed by Müller cells during development[13] and by Müller cells under stress.[55,56] Antibodies against calbindin d28k (CaBP) have

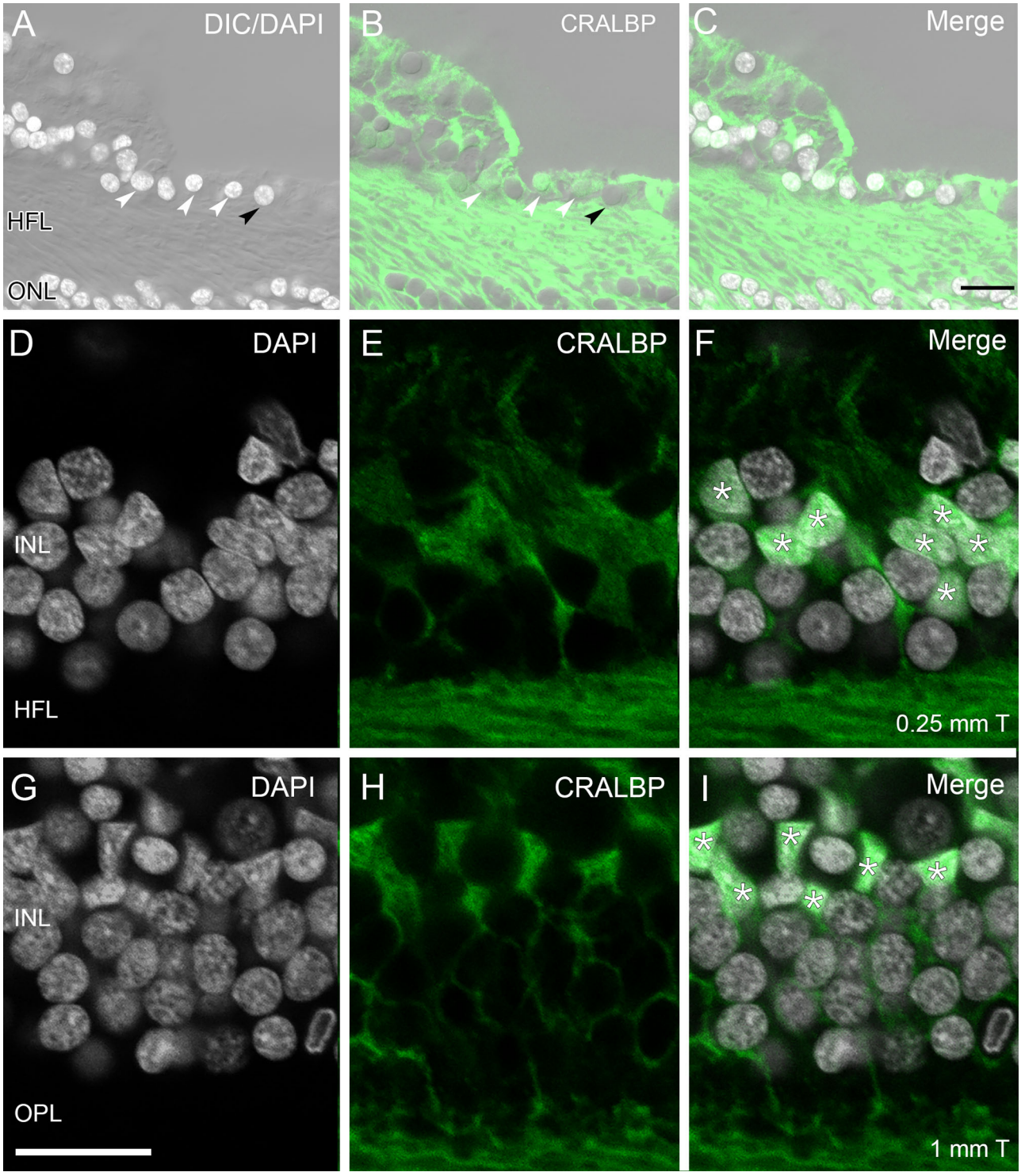

Figure 5. The morphology of Müller cell somas changes with eccentricity. Confocal images of vertical sections through the fovea of a 31-year-old woman (Case no. D19-0859R) taken at different eccentricities. CRALBP-positive Müller cell somas and their inner and outer processes (*green*). DAPI (*white*) and DIC optics reveal the retina layers. (**A–C**) Foveal floor: *White arrowheads* point to round CRALBP-positive somas, *black arrowheads* point to CRALBP-negative somas. (**D–F**) Temporal retina at 0.25 mm eccentricity. CRALBP-positive somas (*asterisks*) are oval shaped. (**G–I**) Temporal retina at 1 mm eccentricity. CRALBP-positive somas (*asterisks*) are polygonal. ONL, outer nuclear layer; HFL, Henle fiber layer; OPL, outer plexiform layer. *Scale bar* shown in **C**: 20 µm applies to **A–C**; *scale bar* shown in **G**: 20 µm applies to **D–I**.

been shown to label subpopulations of cone photoreceptors, horizontal cells, bipolar, amacrine, and ganglion cells in human retina.[33,48,57–62] Antibodies against cone arrestin were used to label cone photoreceptors,[58,63] and antibodies against RNA binding protein with multiple splicing (RBPMS) were used to label retinal ganglion cells.[58,64] Antibodies

Investigative Ophthalmology & Visual Science

against the transient receptor potential vanilloid 4 (TRPV4) cation channel have been shown to label a subpopulation of astrocytes in the mouse brain.[65] In the retina, TRPV4 has been located in Müller cells of mouse[66,67] and in peripheral retina of human[68] and macaque.[69]

Immunofluorescence

Sections (vibratome and cryostat) and the retinal flat mount preparation were processed for standard immunofluorescence as described previously[33,58] using a mixture of primary antibodies. Secondary antibodies (made in donkey) coupled to the fluorophores Alexa 594, Alexa 488 or Alexa 647 (Jackson ImmunoResearch Laboratories, Westgrove, PA, USA) were applied for about 16 hours. The nuclear stain DAPI was added to the diluent for the secondary antibodies. Vibratome sections were mounted onto polylysine-coated slides within wells of adhesive spacers (diameter 20 mm, depth 0.12 mm, secure seal spacers, ThermoFischer Scientific) and then coverslipped with Vectashield aqueous mounting medium (Vector Laboratories, Burlingame, CA, USA).

Microscopy

Tiled stacks of images were obtained from vibratome sections using a confocal scanning microscope (Zeiss LSM700 or LSM900) equipped with 405, 488, 555, and 635 nm lasers using a 20 × air objective (Plan Apochromat no. 420650-9901) at a resolution of 2048 × 2048 or 1024 × 1024 pixels and a Z-axis step size of 0.5–1 µm. Cryostat sections were imaged with a Zeiss LSM800 confocal microscope. The contrast and brightness of the images were adjusted using Zen Blue or Adobe Photoshop software.

Analysis

Cell densities were determined from tiled image stacks using Zen Blue software as described previously.[8,33,58] Briefly, Müller cell nuclei were counted in two preparations (case no. D19-0895R, case no. 13699L) from volumetric reconstructions of Vibratome sections (i.e. by stepping through each image stack and taking the CRALBP immunofluorescence, DAPI, and differential contrast optics into account). Cells were counted across the length and depth of each section, except where the retinal layers were mechanically distorted or the immunolabeling was substantially weaker than in other parts of the same section. Volumetric reconstructions of individual vibratome sections were separated into bins (normally 100 µm width) and cells were counted within each bin across a minimum depth of 15 µm in the z-plane. Areal densities (cells/mm^2 of retinal surface) were calculated for each bin at various eccentricities along the temporal horizontal meridian.

Results

Identification of Cells on the Foveal Floor

Various antibodies were applied to sections through the fovea to investigate the composition of the foveal floor. CRALBP expression was studied in four preparations (no. 13699L, no. 15649L, no. D19-0859R, no. D19-0859L) and was found in the retinal pigment epithelium and in Müller cells, as shown previously.[34,70] The cells were labeled in their entirety including their endfeet forming the inner limiting membrane, their cell bodies in the inner nuclear layer, and their outer processes, which run obliquely within the Henle fiber layer and terminate in the outer limiting membrane (Fig. 1A). For two preparations (no. 13699L and no. D19-0859R) high-resolution confocal images reveal a distinct region at the center of the fovea that has a reduced number of cone nuclei and high density of CRALBP-positive processes (Figs. 1B, 1C). This region spans roughly 70 µm in diameter and presumably represents the central bouquet. Expression of CRALBP is also observed in cell bodies located on the foveal floor among other cell bodies that do not express CRALBP suggesting that not all cells at the foveal floor are Müller cells. In agreement with this interpretation, labeling for the ganglion cell marker, RBPMS, revealed labeled ganglion cells intermingled with Müller cell somas at the foveal floor (Fig. 1D).

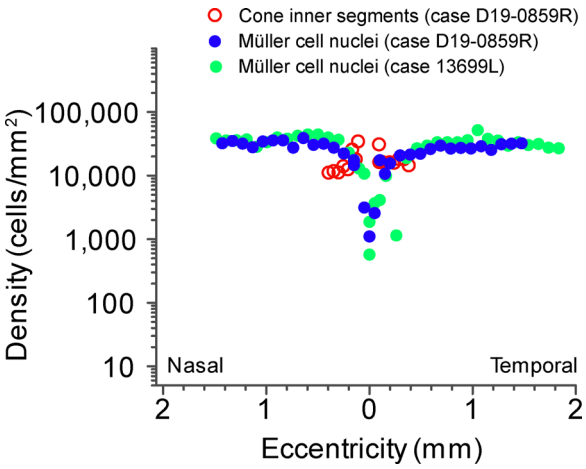

Figure 6. Spatial density of Müller cells. Spatial density of Müller cells quantified from two preparations (D19-0859R, 31-year-old woman and 13699L, 56-year-old man) together with the cone inner segment density obtained from one preparation (D19-0859R). Note that the very central cone inner segments could not be counted in this preparation.

As reported in our previous study,[33] immunofluorescence for GS (Fig. 2A) like that for CRALBP (Fig. 1C) is present at the foveal floor, in the Henle fiber layer, and in processes surrounding cone nuclei in the outer nuclear layer. This result is consistent with the notion that GS is expressed by Müller cells. Two sections (cases no. 13699L and no. D19-0859R) about 200 µm away from the foveal center were stained for GFAP. Here we found a subpopulation of GFAP-positive somas that had inner processes located on the foveal floor (Fig. 2B) but lacked outer processes extending through the outer nuclear layer to the outer limiting membrane (but see below). Taken together our results indicate that the somas located at the foveal floor include glia cells, as well as neurons (ganglion cells).

In addition, we obtained cryostat sections through the fovea from two eyes of two donors following exenteration. These eyes were fixed with a very short delay (see methods). One of the sections from the 86-year-old patient with RPD was double-labeled with antibodies against CRABLP and GFAP, and we found that some but not all somas at the foveal floor coexpressed both markers (Figs. 3A–C). Another section through this retina showed coexpression of GFAP and EAAT4, which is considered an astrocyte marker,[53] in processes at the foveal floor (Figs. 3D–F). In a third section, we found that immunofluorescence for EAAT4 was strongly

Investigative Ophthalmology & Visual Science

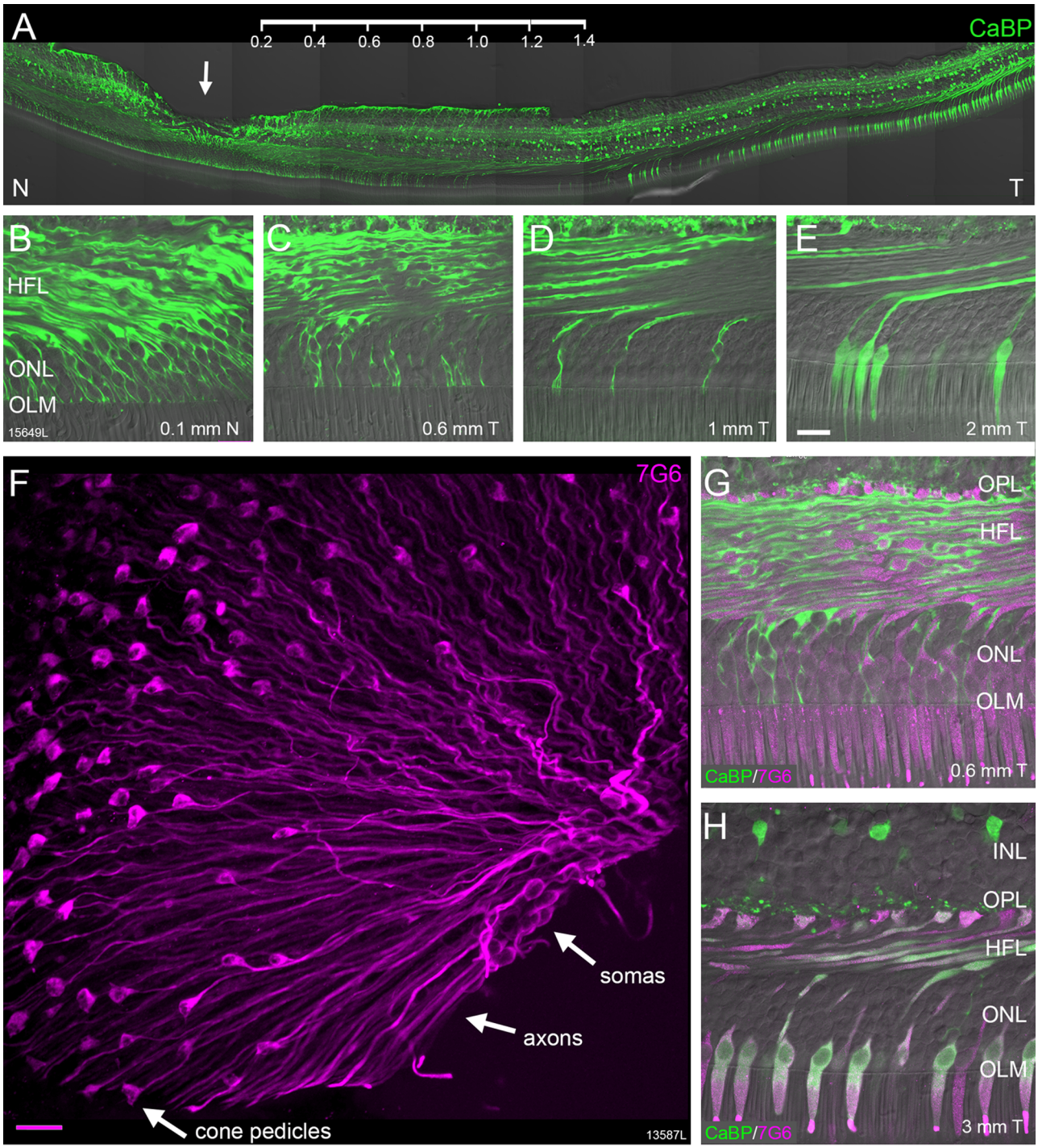

Figure 7. Calbindin expression in foveal Müller cells. (**A–E**, **G**, **H**) Confocal images of a vertical section through the fovea of a 36-year-old female donor (case no. 15649L) processed with antibodies against calbindin (CaBP, *green*). The scale shown in **A** indicates the distance from the fovea in temporal (T) retina. The transitional zone where both calbindin-positive Müller cells and calbindin-positive cone photoreceptors are present is located between 1 and 2 mm eccentricity. (**A–D**) Up to an eccentricity of about 1.2 mm CaBP is expressed almost exclusively by subpopulations of Müller cells, at 2 mm eccentricity CaBP is found in cone photoreceptors (**E**). (**F**) Expression of cone arrestin (7G6) in a foveal flat mount preparation from a 44-year-old female donor (case no. 13587L) showing labeling of cone photoreceptors. The axon terminals (cone pedicles) form a ring around the fovea. The cone axons are displaced from the foveal pit and are part of the Henle fiber layer. The cone somas are located distally from the axons and have short outer processes extending to the cone inner segments. The image was taken in temporal retina. (**G**) At 0.6 mm eccentricity calbindin (*green*) labeled Müller cell processes run alongside cone arrestin (*magenta*) labeled cone axons in the Henle fiber layer (HFL). (**H**) Beyond 1.2 mm eccentricity calbindin (*green*) is coexpressed with cone arrestin (*magenta*) in cone photoceptors including their inner and outer segments, somas, Henle fibers, and cone pedicles. ONL, outer nuclear layer; OPL, outer plexiform layer. *Scale bar* shown in **E**: 20 µm, applies to **B–E**; *scale bar shown* in **F**: 20 µm, applies to **F–H**.

Investigative Ophthalmology & Visual Science

expressed in processes on the foveal floor but was not coexpressed with CRALBP (Figs. 3G–J). Moreover, in a very small region (less than 30 µm in depth) at the center of the fovea, we noticed GFAP-positive processes that extended from the foveal floor through the outer nuclear layer and ended at the outer limiting membrane (Figs. 3A–C, 3J, 3K), indicating that these cells might be the atypical of Müller cells described previously in macaque retina.[16]

Staining of cryostat sections through the fovea from the eye of the 75-year-old patient with no retinal disease revealed similar results. The astrocyte markers EAAT4 and GFAP were coexpressed in cell bodies on the foveal floor and in some processes extending toward the OLM (Figs. 4A–E). Moreover, we found a small region in the center of the fovea that contained GFAP-positive processes extending toward the OLM that were double-labeled for EAAT4 (Figs. 4A–E). In another section we found that some, but not all of these GFAP-positive processes coexpressed the Müller cell marker TPRV4 (Figs. 4F–H). Taken together, we found expression of astrocyte and Müller cell markers on the foveal floor indicating that glial cells on the foveal floor show molecular diversity and may include astrocytes, as well as Müller cells.

Quantification of Müller Cells in the Fovea

Müller cell nuclei immunolabeled for CRALBP were counted in combination with DAPI labeling to distinguish individual nuclei (Fig. 5). Within the foveal floor, Müller cell nuclei have a round shape (Fig. 5A–C), but by −0.2 mm eccentricity the nuclei become more oval shaped (Figs. 5D–F) until gradually the classic polygonal Müller cell nucleus can be appreciated at about 1 mm eccentricity (Figs. 5G–I).

Figure 6 shows the density of CRALBP-positive Müller cell nuclei within the fovea from two preparations (case no. 13699L and case no. D19-0859R) together with the cone density obtained from cone inner segments of a section labeled for cone arrestin (case no. D19-890R). The density of Müller cell nuclei in the fovea did not vary significantly between nasal and temporal retina and was also consistent between the two preparations. The density of CRALBP-positive Müller cell nuclei on the foveal floor was 730 cells/mm^2 in no. 13699L and 1840 cells/mm^2 in no. D19-0859R. The first Müller cell nuclei in the inner nuclear layer (INL) appeared at about 50 µm eccentricity in both nasal and temporal retina. There is a steep increase in the density of Müller cells in the foveal slope with a peak of 35,000 to 40,000 cells/mm^2 at about 500 µm eccentricity. Müller cell density and cone density are roughly equal within the central 1 mm eccentricity in both nasal and temporal retina. Beyond this point, Müller cell density remains relatively stable at around 30,000 cells/mm^2 despite the well-established dramatic decline in cone photoreceptor density across this eccentricity range.[7,58]

Calbindin Expression in Foveal Müller Cells

The calcium binding protein calbindin is known to be expressed in medium- and long-wavelength sensitive (M/L) cone photoreceptors[57] throughout the retina with the exception of the fovea.[48] Here we confirm that calbindin is absent from foveal cones and show that calbindin is expressed by foveal Müller cells (Fig. 7A). This observation was made in five postmortem donor preparations (cases no. 13587R, no. 13699L, no. 15415L, no. 15649L, no. D19-0859R), as well as in the retina from an 86-year-old patient and thus appears to be independent of the age or sex of the donor and of the time interval from death to fixation. The density of calbindin expressing Müller cells declined with increasing eccentricity. For example, in case no. 15649L calbindin expression was found in the large majority of Müller cell outer processes up to an eccentricity of about 0.5 mm (Figs. 7A–C). Beyond this eccentricity calbindin expressing Müller outer processes became less frequent (Fig. 7D). From an eccentricity of about 2 mm calbindin was absent from Müller cells but conversely was expressed in the majority of cones (Fig. 7E). Consistently, sections double labeled with antibodies against cone arrestin (which label cone photoreceptors including their pedicles, Fig. 7F) and calbindin revealed that the outer processes of calbindin labeled Müller cells ensheathe and run in parallel with the cone axons in the Henle fiber layer in foveal retina (Fig. 7G). Beyond 2 mm eccentricity only cones including their axons and pedicles are labeled with both markers (Fig. 7H).

The expression of calbindin in foveal Müller cells was further analyzed in sections double labeled with antibodies against calbindin and CRALBP (cases no. 15649L, no. D19-0859L, no. 13699L). Consistent with the results presented above and shown in Figures 8A–C and 8G–I, close to the center of the fovea calbindin (green) is coexpressed with CRALBP (magenta) in the endfeet, somas, and the Henle fiber layer and at the apical processes of Müller cells. At eccentricities beyond 2 mm, only CRALBP is found in Müller cells, and calbindin is found in cone photoreceptors and subpopulations of amacrine, bipola,r and horizontal cells (Figs. 8D–F, 8J–L). Close inspection of sections through the fovea (Preparations no. 15649L, no. D19-08959R, no. D19-08959L, no. 13699L) further reveals that not all CRALBP positive Müller cell somas are positive for calbindin (Fig. 9).

We attempted to define further the "transitional zone," where calbindin expression in Müller cells overlaps with calbindin expression in cone photoreceptors (Figs. 7A, 7D, 7E; 8J–L). The size for the transitional zone varied somewhat between preparations. For the five preparations (cases no. 13587R, no. 13699L, no. 15415L, no. 15649L, no. D19-0859R) analyzed here, we identified calbindin expressing outer Müller cell processes in the outer nuclear layer at eccentricities up to −1.25 mm (± 0.45 mm) in temporal retina and at eccentricities of about 1.07 mm (± 0.57 mm) in nasal retina. The appearance of the first calbindin labeled cone inner segments ranged from eccentricities of about 0.2 mm to 0.5 mm (average 0.4 mm, ± 0.7 mm, temporal; average 0.4 mm ± 0.2 mm, nasal). Beyond 2.5 mm (± 0.15 mm) calbindin is expressed only by cone photoreceptors. Thus the transitional zone covers approximately 1 mm (Fig. 7A) in both temporal and nasal retina.

The densities of Müller cell somas double labeled for CRALBP and calbindin immuno-fluorescence were quantified in two preparations (Fig. 10) and compared to the total Müller cell density as determined from CRALBP expression (Fig. 6). In both cases, most double labeled cells are found at eccentricities between 0.2 mm and 0.5 mm in both nasal and temporal retina. The proportion of double labeled cells reaches a maximum close to the center of the fovea (96% in preparation no. D19-0859R and 76% in preparation no. 13699L). At about 1 mm eccentricity, the number of double-labeled cells drops below 50% in no. D19-0859R and below 20% in no. 13699L. In summary, calbindin is expressed in a large proportion of foveal Müller cells.

Investigative Ophthalmology & Visual Science

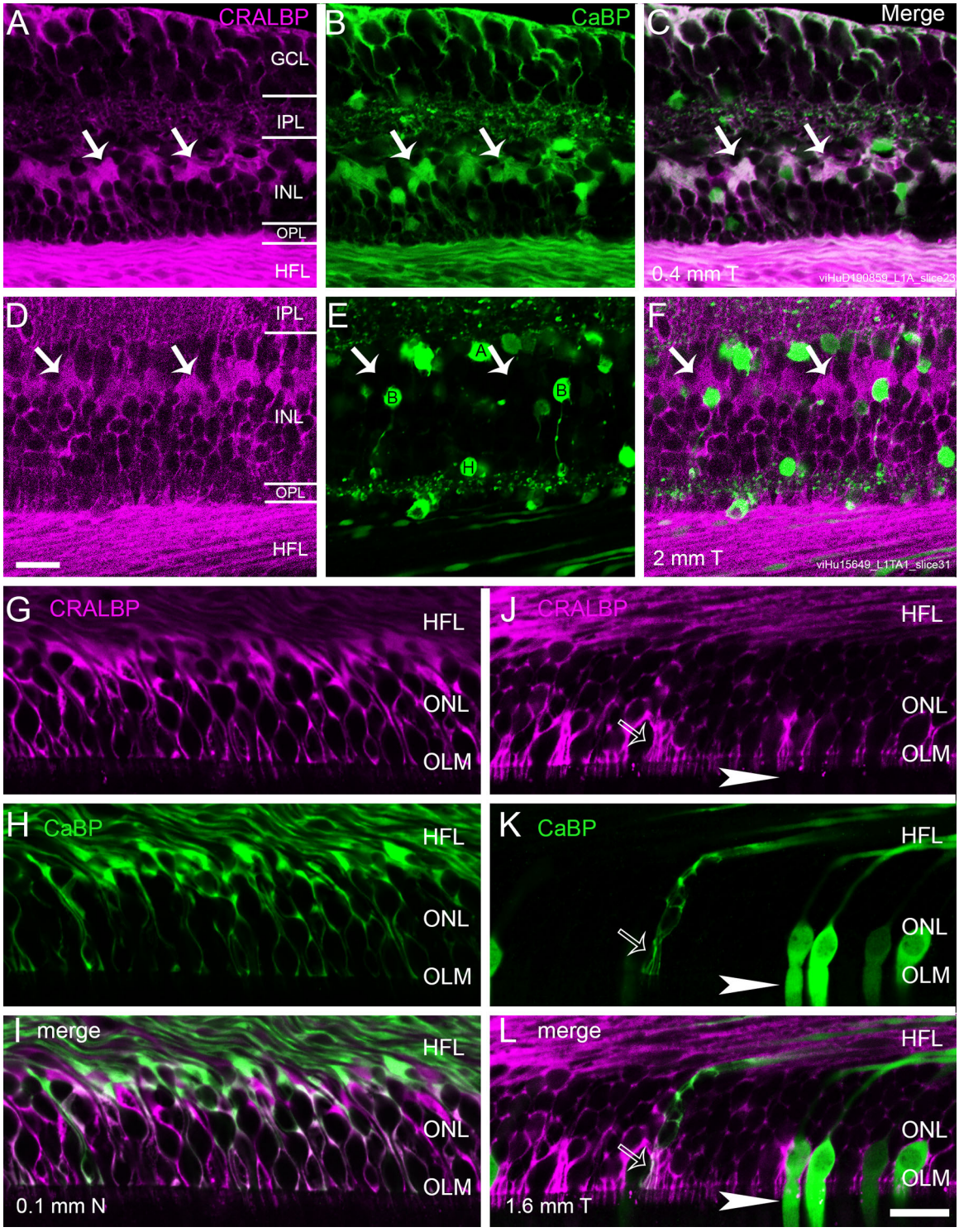

Figure 8. CRALBP and calbindin expression in central and peripheral retina. Confocal images of vertical sections through the fovea of a of a 31-year-old female donor (case no. D19-0859L, **A–C**) and a 36-year-old female donor (case no. 15649L) processed with antibodies against CRALBP (*magenta*) and CaBP (*green*). (**A–C**) Eccentricity 0.4 mm, temporal. CRALP and CaBP are coexpressed in Müller cell somas and endfeet. CaBP is also found in few neurons in the INL and GCL. (**D–F**) Eccentricity 2 mm, temporal. CRALBP and CaBP are not coexpressed. *Arrows* point to CRALBP-positive Müller cell somas. Subpopulations of bipolar (*B*), amacrine (*A*), and horizontal (*H*) cells are also calbindin positive. (**G–I**) Eccentricity 0.1 mm, nasal. CRALBP and CaBP are coexpressed in the outer processes of Müller cells, cones are not labeled for CaBP. (**J–L**) Eccentricity 1.6 mm, temporal. Transitional zone where CaBP expression can be found in subpopulations of cones (*arrowheads*) and Müller cells (*open arrows*). GCL, ganglion cell layer; IPL, inner plexiform layer; ONL, outer nuclear layer; OPL, outer plexiform layer. *Scale bar* shown in **D**: 20 µm, applies to **A–F**; *scale bar* shown in **L**: 20 µm applies to **G–L**.

Investigative Ophthalmology & Visual Science

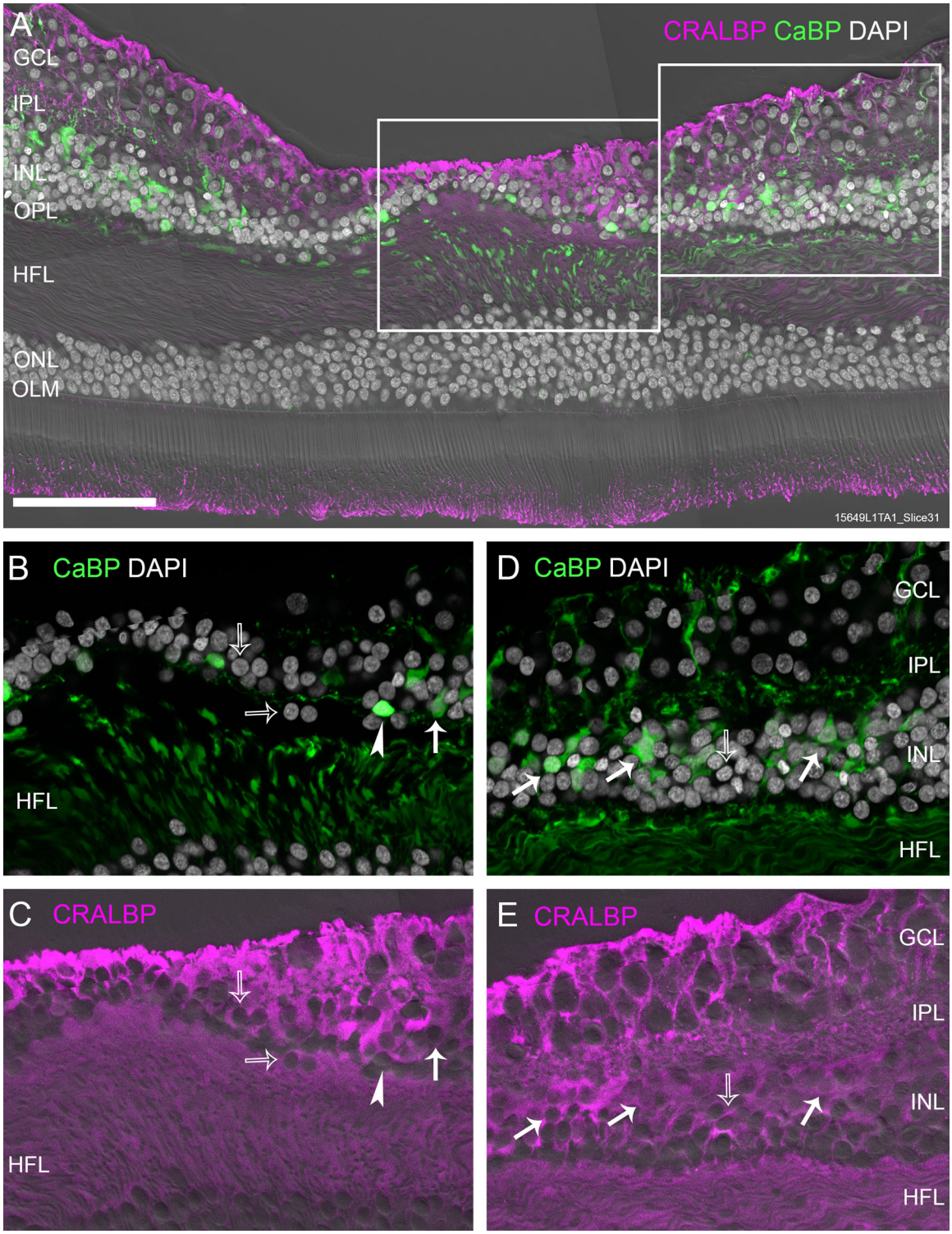

Figure 9. CRALBP and CaBP expression on the foveal floor. Confocal images of sections through the fovea of 36-year-old female donor (case no. 15649L) processed with antibodies against CRALBP (*magenta*) and CaBP (*green*) and counterstained for DAPI. The *rectangles* are 200 µm wide and indicate the regions shown in (**B**, **C**) and (**D**, **E**), respectively. (**B**, **C**) CRALBP is strongly expressed by Müller cell endfeet at the foveal floor and in the HFL. The *white open arrows* indicate cells that are CRALBP-positive but CaBP negative. The *white solid arrowhead* indicates a cell that is CaBP positive but CRALBP negative. (**D**, **E**) CaBP and CRALBP immunofluorescence together with DIC optics to show the retina layers. The two markers are coexpressed in oval shaped Müller cell somas (*solid white arrows*), but some cells are CRALBP positive and CaBP negative (*open arrows*). GCL, ganglion cell layer; IPL, inner plexiform layer; ONL, outer nuclear layer; OPL, outer plexiform layer. *Scale bar*: 100 µm.

Investigative Ophthalmology & Visual Science

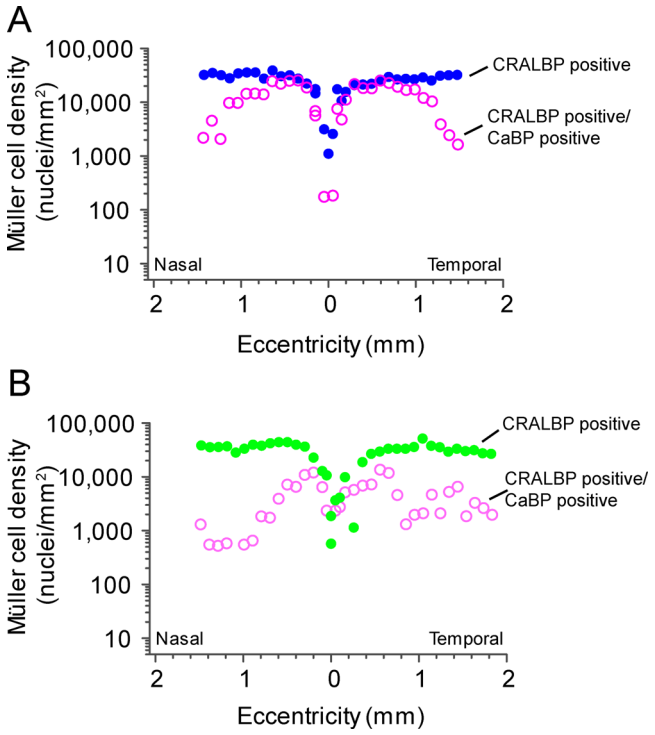

Figure 10. Spatial density of Müller cells that coexpress CRALBP and CaBP (*open circles*) in comparison to all Müller cell nuclei (*solid circles*) for two preparations. (**A**) Case no. D19-0895R, 31-year-old woman); (**B**) case no. 13699L, 56-year-old man).

Coexpression of Calbindin With Other Glia Markers in the Fovea

The molecular properties of calbindin-expressing Müller cells in the fovea were further investigated in sections double labeled for calbindin and the glia markers GFAP (Fig. 11) and GS (Fig. 12). As expected,[13,14] outside of the foveal center GFAP immunofluorescence was associated with blood vessels (arrows in Fig. 11C) and clearly distinct from calbindin expression (Figs. 11A, 11B) and CRALBP expression (Fig. 1A) consistent with the idea that GFAP is expressed in astrocytes. Calbindin was coexpressed with glutamine synthetase in most but not all Müller cells of central retina (Fig. 12). This finding is consistent with the results obtained with CRALBP antibodies described above.

Discussion

This study has three major findings. First, we confirm and extend previous findings showing that the foveal floor in human retina contains somas of neurons and glial cells. Second, we show that in the foveal retina there is at least one Müller cell per cone. Third, we demonstrate that the large majority of Müller cells in the fovea express the calcium binding protein calbindin and thus foveal Müller cells differ in their molecular properties from Müller cells in peripheral retina. The qualitative results are summarized in Fig. 13.

The presence of retinal ganglion cell somas in the center of the human fovea has been reported previously[71] and is also consistent with previous studies of nonhuman primates[23,72–75] suggesting that this is a normal part of foveal architecture. Other neuronal somas found on the foveal floor include horizontal,[76] amacrine,[77] and bipolar cells.[78] Whether the neurons on the foveal floor are remnants of foveal development or have a specific functional role remains unknown.[2]

In the present study, glia cell labeling in the foveal center included immunofluorescence for Müller cell markers (CRALBP, GS, and TRPV4) and for astrocyte markers (GFAP and EAAT4). The presence of Müller cells in the fovea is well documented for healthy human and macaque monkey retinas,[11,15,23,70] and thus our results support these previous studies.

Whether the GFAP-expressing cells on the foveal floor are Müller cells or astrocytes is controversial. Bringmann and colleagues[11,16] reported coexpression of GFAP and GS in somas and outer processes of cells in the center of a macaque fovea and suggested that these cells represent the atypical Müller cells described in their previous EM study.[24] In human retina, we observed GFAP expression in somas and inner processes at the foveal floor in postmortem as well as in the two fresh preparations (Figs. 2, 3A–F, 4). GFAP positive outer processes, however, were only observed in a very small region at the center of the fovea of the two freshly obtained human retinas (Figs. 3J, 3K, 4F–H). These outer processes were probably missed in our GFAP-labeled vibratome sections of postmortem retina, because these sections were taken at about 200 µm away from the center of the fovea. The presence of outer GFAP positive processes and the coexpression with CRALBP are consistent with the idea that these cells are Müller cells. We cannot rule out that GFAP expression by Müller cells in the RPD retina is due to gliosis.[55,56] However, the retina of the 75-year-old patient without retinal disease showed comparable GFAP expression on the foveal floor suggesting that GFAP might be expressed by non-gliotic Müller cells in the fovea.

In contrast, two recent studies applied GFAP antibodies in combination with a variety of Müller cell markers to foveal sections of adult macaque monkeys[39] and humans[38] and found that the GFAP labeled cells in the foveola did not co-express a variety of Müller cell markers. These studies thus concluded that the GFAP positive cells in the foveola are astrocytes. Consistent with the latter conclusion, we found co-expression of GFAP with the astrocyte marker EAAT4 (Figs. 3D–F; 4A–E). The conclusion that astrocytes are present in the foveola seems at odds with the assumption that astrocytes are absent from the foveal avascular zone.[13,79–81] However, GFAP labeled astrocytes in the center of the fovea are present during development and, in adult macaque monkey, a few astrocytes were found in the middle of the fovea.[81] Thus it is possible that foveal astrocytes, like their neuronal counterparts, are unmigrated remnants of foveal development.

Finally, we show that TRPV4 is expressed in some but not all processes in the foveola of the 75-year-old patient without eye disease (Fig. 4F–H). In the retina, TRPV4 is thought to be a marker for Müller cells and has been implicated with osmoregulation, mechanotransduction and regulation of the inner and outer blood brain barrier.[82] TRPV4 also plays a role in ganglion cell recovery after mechanical insult[67] Thus its presence in the fovea is consistent with the idea that foveal Müller cells are involved in the response to mechanical stress.[47] The fact that GFAP and TRPV4 immunolabel do not overlap completely might indicate that that in addition to these specialized Müller cells the fovea also contains astrocytes which (in studies of higher brain regions) recently have been shown to be more diverse than previously expected.[83]

Investigative Ophthalmology & Visual Science

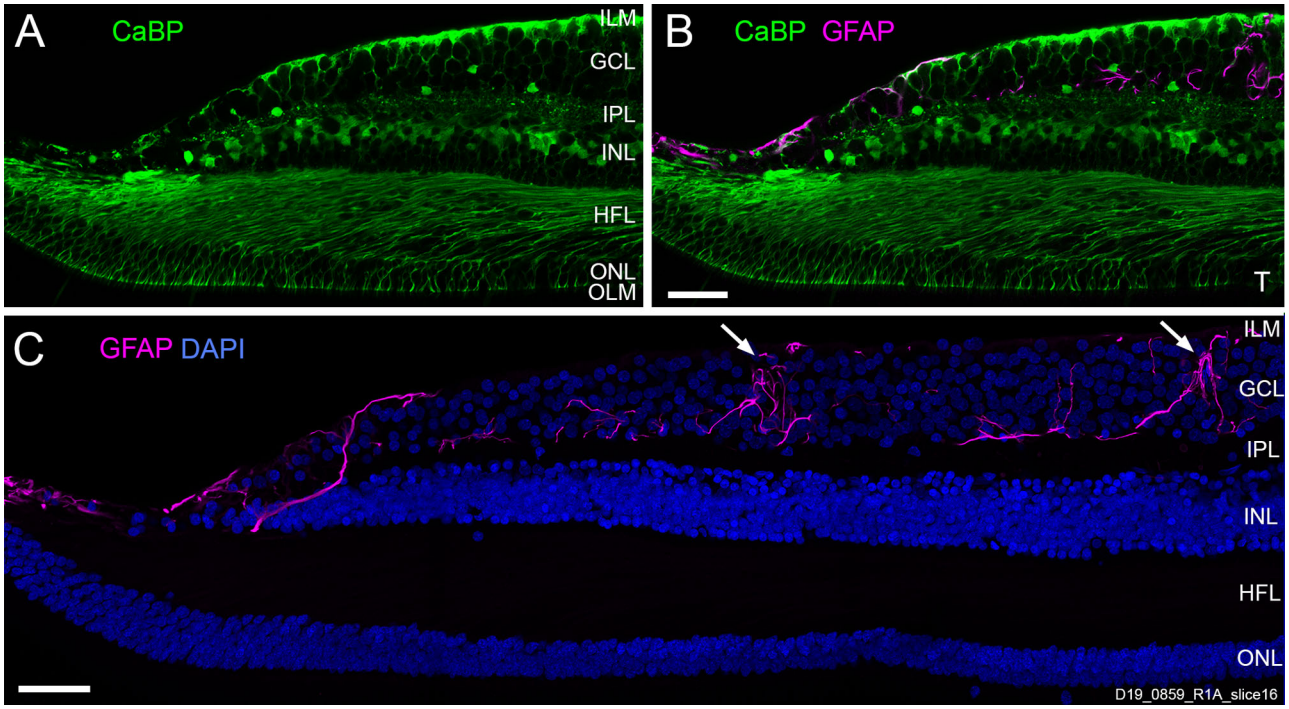

Figure 11. Calbindin and GFAP in the fovea. Confocal images of a vertical section through the fovea of a 31-year-old female donor (case no. D19-0859L). The section was processed for CaBP (*green*), GFAP (*magenta*), and DAPI (*blue*). (**A**) CaBP expression in foveal Müller cells. (**B**) Merged image showing CaBP together with GFAP. GFAP is mainly found in the ganglion cell layer (GCL) and in the nerve fiber layer near the Müller cell endfeet. **A** and **B** show single images from a stack of images. (**C**) Maximum intensity projection of confocal images from a stack of images of the same section as shown in **A**, **B** revealing the morphology of GFAP positive astrocytes in the fovea. The *arrows* point to blood vessels. ONL, outer nuclear layer; IPL, inner plexiform layer. *Scale bar*: 50 µm.

Taken together, the current evidence, together with the finding of sparse microglia on the foveal floor,[84] suggest that the foveola contains at least three types of glia (Müller cells, astrocytes and microglia) and that Müller cells are by far the dominant glial population in the foveola.

In the present study we counted CRALBP positive Müller cell nuclei and found a peak density of about 35,000 Müller cells/mm^2 near 0.5 mm eccentricity in both nasal and temporal retina. Comparable values (average 24,000 cells/mm^2 at 1 mm eccentricity) were obtained in our previous study where we counted GS positive Müller cell nuclei in temporal retina.[33] Somewhat lower values (around 15,000 cells/mm^2) were reported by Bringmann et al.[16] who counted stems of Müller cells in the outer nuclear layer and the inner plexiform layer (see their figure 15B). A recent connectomics study of a preterm born 28-year-old male human donor[85] reported a peak density of about 25,000 cells/mm^2 from counting Müller cell somas in the INL near the foveola. In summary, all three previous studies and the current study obtained roughly comparable Müller cell densities.

Kar and colleagues' study[85] of a preterm born adult, which had a foveal center containing inner retinal layers, reports considerably higher Müller cell densities (200,000 cells/mm^2) when Müller cell trunks were counted close to the region of the peak cone density.[85] But the peak cone density obtained in that study is comparable to previous studies of normal human retina[7,58] Thus the cone to Müller cell ratio of 1:1.8 in the preterm born adult is comparable to previous estimates of 1 to 2 Müller cells per cone for human[16,33] and macaque retina,[31] indicating that this ratio was not affected by the arrested development in a preterm born adult donor.

It should be noted that the study of the preterm born adult male in addition to the classic Müller cells also reports a second (atypical) Müller cell type, named "inner" Müller glia.[85] These inner Müller cells, like the classic ("outer") Müller cells, have a soma in the inner nuclear layer but their outer processes terminate at the level of the cone pedicles. The inner Müller cells are thus different from the small number of atypical Müller cells in the foveola described previously which were reported to extend to the OLM.[16] The inner Müller cells were twice as frequent as outer Müller cells and together the two populations outnumbered cones by fourfold. Whether these "inner" Müller cells are present in normal retina or are the result of arrested development of the inner retinal neurons in the preterm retina needs further investigation.

Calbindin expression in Müller cells has been identified in RNAseq studies of adult human retina[42] and using immunofluorescence staining of foveal sections through human retina during development.[86] Here we found that in foveal retina a large proportion of Müller cells expresses calbindin whereas at eccentricities beyond 1 mm the expression of calbindin is only found in a small portion of Müller cells. Haley and coworkers[48] noticed calbindin staining in the Henle fiber layer in the fovea of adult human retina. They interpreted that staining as cone axon labeling despite its absence from cone inner and outer segments. Taking our results in account, it appears likely that the labeling in the Henle fiber layer found by Haley and coworkers[48] should be attributed to Müller cell processes. Calbindin

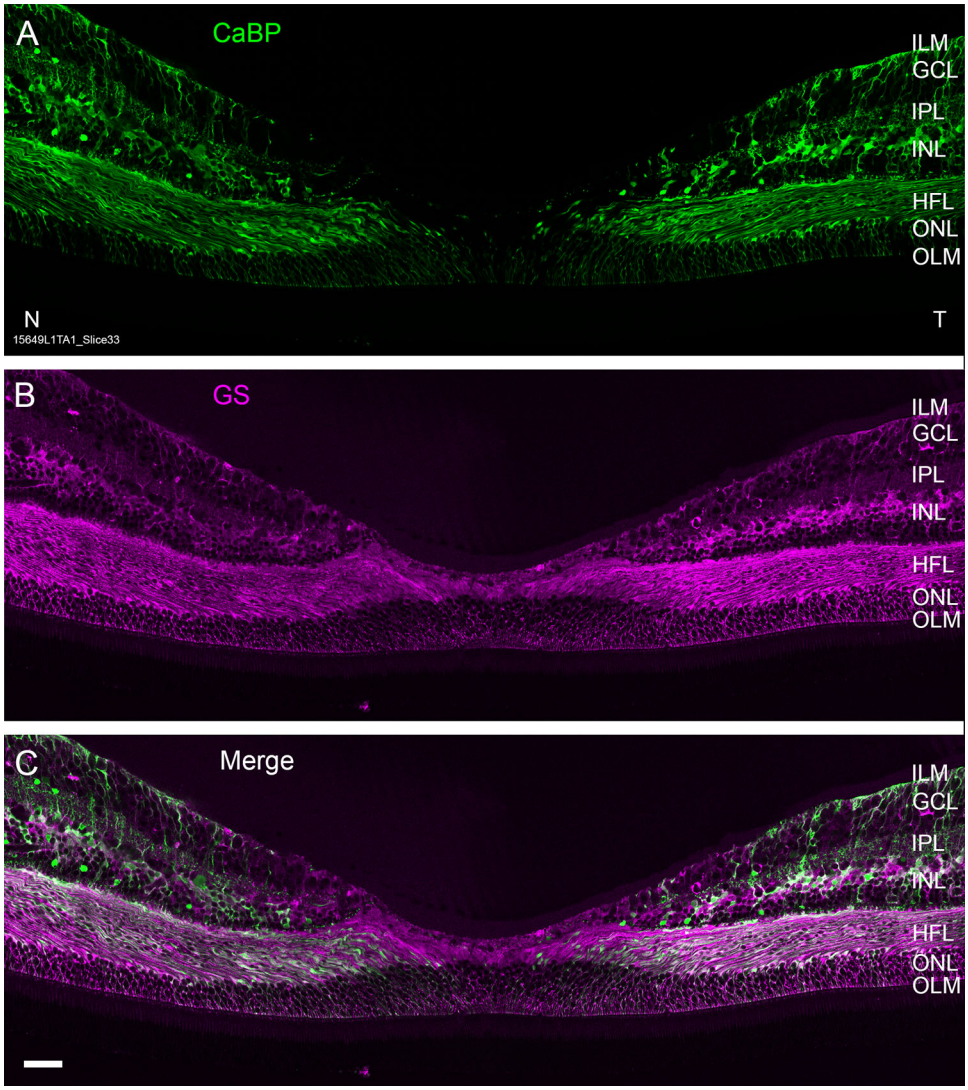

Figure 12. Calbindin and glutamine synthetase in the fovea. Confocal images of a vertical section through the fovea of a 36-year-old female donor (case no. 15649L) processed for CaBP (*green*) and GS (*magenta*) showing coexpression of the two markers in Müller cells. GCL, ganglion cell layer; IPL, inner plexiform layer; N, nasal; ONL, outer nuclear layer; T, temporal. *Scale bar*: 50 µm.

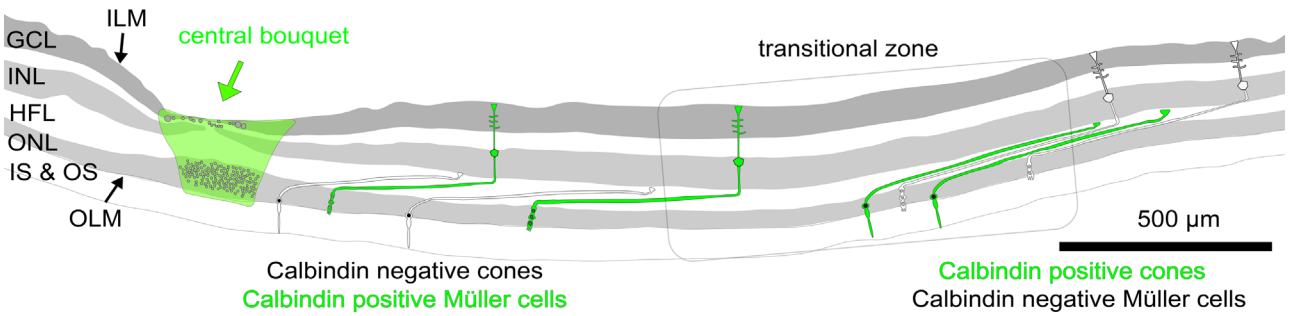

Figure 13. Summary diagram of our qualitative results. Semi-schematic drawing of the section through the macula of preparation no. 15649L. The original image is shown in Figure 7A. The area highlighted in *green* refers to the central bouquet, which contains many calbindin- and CRALBP-positive processes in addition to cone photoreceptors. The somas on the foveal floor (shown in *gray*) comprise glial and neuronal cells. Close to the center of the fovea most Müller cells are calbindin positive, and cones are calbindin negative. In the peripheral region of the macula Müller cells are calbindin negative, but nearly all cones are calbindin positive. The *gray rectangle* indicates the transitional zone where both calbindin-positive Müller cells and calbindin-positive cones can be found. GCL, ganglion cell layer; IS, inner segment of photoreceptors; ONL, outer nuclear layer; OS, outer segment of photoreceptors.

Investigative Ophthalmology & Visual Science

like other calcium binding proteins plays a role in calcium buffering[87] and calbindin is usually found in neurons where it contributes to the regulation of electrical excitability.[88] Calbindin expression has also been seen in astrocytes in the brain after injury and thus has been suggested to have a neuroprotective role.[89,90] The role of calbindin in foveal Müller cells, however, remains to be determined.

Other evidence supporting differences between central and peripheral Müller cells in human retina comes from molecular studies showing differences in gene and protein expression[20,44–47] and from biochemical studies showing differences in the response to stress between macular and peripheral Müller cells.[91] In Macular Telangiectasia Type 2 (MacTel), a retinal degenerative disease, Müller cells degenerate within an oval shaped zone of 2.5 to 3 mm, which includes the fovea (MacTel zone).[92–94] In all these studies the region where central Müller cells differ from peripheral Müller cells coincides with the presence and absence of calbindin expression, respectively, suggesting that calbindin expression, in some as-yet unknown way, contributes to the susceptibility of the macula to retinal disease.[91] An alternative (but not mutually exclusive) hypothesis is suggested by the fact that the region of calbindin expression coincides with the macula lutea, which is a region rich in xanthophyll carotenoids.[85] This association could link calbindin expression to cone resilience and foveal sparing in disease and aging.[95,96]

Acknowledgments

The authors thank Ling Zhou, Ting Zhang, and Nasir Uddin for advice and sharing antibodies, Alyssa Baldicano for excellent technical assistance, and the Lions NSW Eye Bank and Australian Ocular Biobank for providing postmortem eye tissue. The authors also thank the editors and anonymous reviewers for many helpful comments and suggestions.

Supported by Project Grant APP1123418 from the National Health & Medical Research Council (U.G. and P.R.M.)

Disclosure: **R.A. Masri**, None; **U. Greferath**, None; **E.L. Fletcher**, None; **P.R. Martin**, None; **U. Grünert**, None

References

1. Hendrickson A. Organization of the adult primate fovea. In: Penfold PL, Provis JM, eds. *Macular degeneration*. Berlin: Springer; 2005.
2. Provis JM, Díaz CM, Dreher B. Ontogeny of the primate fovea: a central issue in retinal development. *Prog Neurobiol*. 1998;54:549–581.
3. Provis JM, Dubis AM, Maddess T, Carroll J. Adaptation of the central retina for high acuity vision: cones, the fovea and the avascular zone. *Prog Retin Eye Res*. 2013;35:63–81.
4. Quinn N, Csincsik L, Flynn E, et al. The clinical relevance of visualising the peripheral retina. *Prog Retin Eye Res*. 2019;68:83–109.
5. Østerberg GA. Topography of the layer of rods and cones in the human retina. *Acta Ophthalmol (Copenh)*. 1935;6:1–102.
6. Packer O, Hendrickson AE, Curcio CA. Photoreceptor topography of the adult pigtail macaque (Macaca nemestrina). *J Comp Neurol*. 1989;288:165–183.
7. Curcio CA, Sloan KR, Kalina RE, Hendrickson AE. Human photoreceptor topography. *J Comp Neurol*. 1990;292:497–523.
8. Lee SCS, Martin PR, Grünert U. Topography of neurons in the rod pathway of human retina. *Invest Ophthalmol Vis Sci*. 2019;60:2848–2859.
9. Snodderly DM, Weinhaus RS, Choi JC. Neural-vascular relationships in central retina of macaque monkeys (Macaca fascicularis). *J Neurosci*. 1992;12:1169–1193.
10. Dubis AM, Hansen BR, Cooper RF, Beringer J, Dubra A, Carroll J. Relationship between the foveal avascular zone and foveal pit morphology. *Invest Ophthalmol Vis Sci*. 2012;53:1628–1636.
11. Bringmann A, Unterlauft JD, Barth T, Wiedemann R, Rehak M, Wiedemann P. Müller cells and astrocytes in tractional macular disorders. *Prog Retin Eye Res*. 2022;86:100977.
12. Daruich A, Matet A, Moulin A, et al. Mechanisms of macular edema: Beyond the surface. *Prog Retin Eye Res*. 2018;63:20–68.
13. Provis JM, Sandercoe T, Hendrickson AE. Astrocytes and blood vessels define the foveal rim during primate retinal development. *Invest Ophthalmol Vis Sci*. 2000;41:2827–2836.
14. Distler C, Weigel H, Hoffmann K-P. Glia cells of the monkey retina. I. Astrocytes. *J Comp Neurol*. 1993;333:134–147.
15. Distler C, Dreher Z. Glia cells of the monkey retina. II. Müller cells. *Vision Res*. 1996;36:2381–2394.
16. Bringmann A, Syrbe S, Görner K, et al. The primate fovea: Structure, function and development. *Prog Ret Eye Res*. 2018;66:49–84.
17. Carpi-Santos R, de Melo Reis RA, Gomes FCA, Calaza KC. Contribution of Müller Cells in the Diabetic Retinopathy Development: Focus on Oxidative Stress and Inflammation. *Antioxidants (Basel)*. 2022;11:617.
18. Edwards MM, McLeod DS, Bhutto IA, Villalonga MB, Seddon JM, Lutty GA. Idiopathic preretinal glia in aging and age-related macular degeneration. *Exp Eye Res*. 2016;150:44–61.
19. Edwards MM, McLeod DS, Bhutto IA, Grebe R, Duffy M, Lutty GA. Subretinal Glial Membranes in Eyes With Geographic Atrophy. *Invest Ophthalmol Vis Sci*. 2017;58:1352–1367.
20. Menon M, Mohammadi S, Davila-Velderrain J, et al. Single-cell transcriptomic atlas of the human retina identifies cell types associated with age-related macular degeneration. *Nat Commun*. 2019;10:4902.
21. Jorstad NL, Wilken MS, Grimes WN, et al. Stimulation of functional neuronal regeneration from Müller glia in adult mice. *Nature*. 2017;548:103–107.
22. Jui J, Goldman D. Müller Glial Cell-Dependent Regeneration of the Retina in Zebrafish and Mice. *Annu Rev Genet*. 2024;58:67–90.
23. Polyak SL. *The Retina*. Chicago: The University of Chicago Press; 1941
24. Syrbe S, Kuhrt H, Gärtner U, et al. Müller glial cells of the primate foveola: An electron microscopical study. *Exp Eye Res*. 2018;167:110–117.
25. Reichenbach A, Bringmann A. Glia of the human retina. *Glia*. 2020;68:768–796.
26. Reichenbach A, Bringmann A. Müller cells in the healthy retina. In: Reichenbach A, Bringmann A, eds. *Müller Cells in the Healthy and Diseased Retina*. New York, NY: Springer; 2010
27. Wang J, O'Sullivan ML, Mukherjee D, Puñal VM, Farsiu S, Kay JN. Anatomy and spatial organization of Müller glia in mouse retina. *J Comp Neurol*. 2017;525:1759–1777.
28. Yamada E. Some structural features of the fovea centralis in the human retina. *Arch Ophthalmol*. 1969;82:151–159.
29. Gass JD. Müller cell cone, an overlooked part of the anatomy of the fovea centralis: hypotheses concerning its role in the pathogenesis of macular hole and foveomacualr retinoschisis. *Arch Ophthalmol*. 1999;117:821–823.

30. Govetto A, Bhavsar KV, Virgili G, et al. Tractional Abnormalities of the Central Foveal Bouquet in Epiretinal Membranes: Clinical Spectrum and Pathophysiological Perspectives. *Am J Ophthalmol*. 2017;184:167–180.
31. Burris C, Klug K, Ngo IT, Sterling P, Schein S. How Müller glial cells in macaque fovea coat and isolate the synaptic terminals of cone photoreceptors. *J Comp Neurol*. 2002;453:100–111.
32. Ahmad KM, Klug K, Herr S, Sterling P, Schein S. Cell density ratios in a foveal patch in macaque retina. *Visual Neurosci*. 2003;20:189–209.
33. Masri RA, Weltzien F, Purushothuman S, Lee SCS, Martin PR, Grünert U. Composition of the Inner Nuclear Layer in Human Retina. *Invest Ophthalmol Vis Sci*. 2021;62:22.
34. Bunt-Milam AH, Saari JC. Immunocytochemical localization of two retinoid-binding proteins in vertebrate retina. *J Cell Biol*. 1983;97:703–712.
35. Kolesnikov AV, Kiser PD, Palczewski K, Kefalov VJ. Function of mammalian M-cones depends on the level of CRALBP in Müller cells. *J Gen Physiol*. 2021;153: e202012675.
36. Bassetto M, Kolesnikov AV, Lewandowski D, et al. Dominant role for pigment epithelial CRALBP in supplying visual chromophore to photoreceptors. *Cell Rep*. 2024;43: 114143.
37. Hendrickson A, Possin D, Vajzovic L, Toth CA. Histologic development of the human fovea from midgestation to maturity. *Am J Ophthalmol*. 2012;154:767–778.e2.
38. Delaunay K, Khamsy L, Kowalczuk L, et al. Glial cells of the human fovea. *Mol Vis*. 2020;26:235–245.
39. Ikeda T, Nakamura K, Oku H, Horie T, Kida T, Takai S. Immunohistological Study of Monkey Foveal Retina. *Sci Rep*. 2019;9:5258.
40. Matet A, Savastano MC, Rispoli M, et al. En face optical coherence tomography of foveal microstructure in full-thickness macular hole: a model to study perifoveal Müller cells. *Am J Ophthalmol*. 2015;159:1142–1151.e3.
41. Nishikawa S, Tamai M. Müller cells in the human foveal region. *Curr Eye Res*. 2001;22:34–41.
42. Yan W, Peng YR, van Zyl T, et al. Cell Atlas of The Human Fovea and Peripheral Retina. *Scientific Reports*. 2020;10:9802.
43. Peng YR, Shekhar K, Yan W, et al. Molecular classification and comparative taxonomics of foveal and peripheral cells in primate retina. *Cell*. 2019;176:1222–1237.
44. Cowan CS, Renner M, De Gennaro M, et al. Cell Types of the Human Retina and Its Organoids at Single-Cell Resolution. *Cell*. 2020;182:1623–1640.e34.
45. Lu Y, Shiau F, Yi W, et al. Single-Cell Analysis of Human Retina Identifies Evolutionarily Conserved and Species-Specific Mechanisms Controlling Development. *Dev Cell*. 2020;53:473–491.e9.
46. Voigt AP, Mullin NK, Whitmore SS, et al. Human photoreceptor cells from different macular subregions have distinct transcriptional profiles. *Hum Mol Genet*. 2021;30:1543–1558.
47. Kaplan L, Drexler C, Pfaller AM, et al. Retinal regions shape human and murine Müller cell proteome profile and functionality. *Glia*. 2023;71:391–414.
48. Haley TL, Pochet R, Baizer L, et al. Calbindin D-28K immunoreactivity of human cone cells varies with retinal position. *Visual Neurosci*. 1995;12:301–307.
49. FitzGibbon T, Nestorovski Z. Morphological consequences of myelination in the human retina. *Exp Eye Res*. 1997;65:809–819.
50. Greferath U, Guymer RH, Vessey KA, Brassington K, Fletcher EL. Correlation of Histologic Features with In Vivo Imaging of Reticular Pseudodrusen. *Ophthalmology*. 2016;123:1320–1331.
51. Bringmann A, Pannicke T, Grosche J, et al. Müller cells in the healthy and diseased retina. *Prog Retin Eye Res*. 2006;25:397–424.
52. Riepe RE, Norenburg MD. Müller cell localisation of glutamine synthetase in rat retina. *Nature*. 1977;268:654–655.
53. Ward MM, Jobling AI, Puthussery T, Foster LE, Fletcher EL. Localization and expression of the glutamate transporter, excitatory amino acid transporter 4, within astrocytes of the rat retina. *Cell Tissue Res*. 2004;315:305–310.
54. Hu WH, Walters WM, Xia XM, Karmally SA, Bethea JR. Neuronal glutamate transporter EAAT4 is expressed in astrocytes. *Glia*. 2003;44:13–25.
55. Milam AH, Li ZY, Fariss RN. Histopathology of the human retina in retinitis pigmentosa. *Prog Retin Eye Res*. 1998;17:175–205.
56. Dyer MA, Cepko CL. Control of Müller glial cell proliferation and activation following retinal injury. *Nat Neurosci*. 2000;3:873–880.
57. Chiquet C, Dkhissi-Benyahya O, Chounlamountri N, Szel A, Degrip WJ, Cooper HM. Characterization of calbindin-positive cones in primates. *Neuroscience*. 2002;115:1323–1333.
58. Masri RA, Grünert U, Martin PR. Analysis of parvocellular and magnocellular visual pathways in human retina. *J Neurosci*. 2020;40:8132–8148.
59. Haverkamp S, Haeseleer F, Hendrickson A. A comparison of immunocytochemical markers to identify bipolar cell types in human and monkey retina. *Visual Neurosci*. 2003;20:589–600.
60. Chandra AJ, Lee SCS, Grünert U. Melanopsin and calbindin immunoreactivity in the inner retina of humans and marmosets. *Visual Neurosci*. 2019;36:E009.
61. Hendrickson A, Yan YH, Erickson A, Possin D, Pow D. Expression patterns of calretinin, calbindin and parvalbumin and their colocalization in neurons during development of Macaca monkey retina. *Exp Eye Res*. 2007;85:587–601.
62. Craft CM, Huang J, Possin DE, Hendrickson A. Primate short-wavelength cones share molecular markers with rods. *Adv Exp Med Biol*. 2014;801:49–56.
63. Zhang H, Cuenca N, Ivanova T, et al. Identification and light-dependent translocation of a cone-specific antigen, cone arrestin, recognized by monoclonal antibody 7G6. *Invest Ophthalmol Vis Sci*. 2003;44:2858–2867.
64. Rodriguez AR, Pérez de Sevilla Müller L, Brecha NC. The RNA binding protein RBPMS is a selective marker of ganglion cells in the mammalian retina. *J Comp Neurol*. 2014;522:1411–1443.
65. Shibasaki K, Ikenaka K, Tamalu F, Tominaga M, Ishizaki Y. A novel subtype of astrocytes expressing TRPV4 (transient receptor potential vanilloid 4) regulates neuronal excitability via release of gliotransmitters. *J Biol Chem*. 2014;289:14470–14480.
66. Jo AO, Ryskamp DA, Phuong TT, et al. TRPV4 and AQP4 Channels Synergistically Regulate Cell Volume and Calcium Homeostasis in Retinal Müller Glia. *J Neurosci*. 2015;35:13525–13537.
67. Lee PY, Greferath U, Zhao D, et al. Systemic TRPV4 inhibition worsens retinal response to acute IOP elevation in older but not younger mice. *Optom Vis Sci*. 2025;in press
68. Ryskamp DA, Jo AO, Frye AM, et al. Swelling and eicosanoid metabolites differentially gate TRPV4 channels in retinal neurons and glia. *J Neurosci*. 2014;34:15689–15700.
69. Gao F, Yang Z, Jacoby RA, Wu SM, Pang JJ. The expression and function of TRPV4 channels in primate retinal ganglion cells and bipolar cells. *Cell Death Dis*. 2019;10: 364.

Investigative Ophthalmology & Visual Science

70. Cuenca N, Ortuño-Lizarán I, Pinilla I. Cellular Characterization of OCT and Outer Retinal Bands Using Specific Immunohistochemistry Markers and Clinical Implications. *Ophthalmology*. 2018;125:407–422.
71. Curcio CA, Allen KA. Topography of ganglion cells in human retina. *J Comp Neurol*. 1990;300:5–25.
72. Grünert U, Greferath U, Boycott BB, Wässle H. Parasol (Pα) ganglion cells of the primate fovea: Immunocytochemical staining with antibodies against GABAA receptors. *Vision Res*. 1993;33:1–14.
73. Bunt AH, Minckler DS, Johanson GW. Demonstration of bilateral projection of the central retina of the monkey with horseradish peroxidase neuronography. *J Comp Neurol*. 1977;171:619–630.
74. Leventhal AG, Ault SJ, Vitek DJ, Shou T. Extrinsic determinants of retinal ganglion cell development in primates. *J Comp Neurol*. 1989;286:170–189.
75. Leventhal AG, Thompson KG, Liu D. Retinal ganglion cells within the foveola of New World (*Saimiri sciureus*) and Old World (*Macaca fascicularis*) monkeys. *J Comp Neurol*. 1993;338:242–254.
76. Röhrenbeck J, Wässle H, Boycott BB. Horizontal cells in the monkey retina: immunocytochemical staining with antibodies against calcium binding proteins. *Eur J Neurosci*. 1989;1:407–420.
77. Savy C, Simon A, Nguyen-Legros J. Spatial geometry of the dopamine innervation in the avascular area of the human fovea. *Vis Neurosci*. 1991;7:487–498.
78. Grünert U, Martin PR, Wässle H. Immunocytochemical analysis of bipolar cells in the macaque monkey retina. *J Comp Neurol*. 1994;348:607–627.
79. Gariano RF, Sage EH, Kaplan HJ, Hendrickson AE. Development of astrocytes and their relation to blood vessels in fetal monkey retina. *Invest Ophthalmol Vis Sci*. 1996;37:2367–2375.
80. Triviño A, Ramírez JM, Salazar JJ, Ramírez AI. Human retinal astroglia. A comparative study of adult and the 18 month postnatal developmental stage. *J Anat*. 2000;196:61–70.
81. Distler C, Kopatz K, Telkes I. Developmental changes in astrocyte density in the macaque perifoveal region. *Eur J Neurosci*. 2000;12:1331–1341.
82. Križaj D, Cordeiro S, Strauß O. Retinal TRP channels: Cell-type-specific regulators of retinal homeostasis and multimodal integration. *Prog Retin Eye Res*. 2023;92:101114.
83. Murphy-Royal C, Ching S, Papouin T. A conceptual framework for astrocyte function. *Nat Neurosci*. 2023;26:1848–1856.
84. Singaravelu J, Zhao L, Fariss RN, Nork TM, Wong WT. Microglia in the primate macula: specializations in microglial distribution and morphology with retinal position and with aging. *Brain Struct Funct*. 2017;222:2759–2771.
85. Kar D, Singireddy R, Kim YJ, et al. Unusual morphology of foveal Müller glia in an adult human born pre-term. *Front Cell Neurosci*. 2024;18:1409405.
86. Zhang C, Yu WQ, Hoshino A, et al. Development of ON and OFF cholinergic amacrine cells in the human fetal retina. *J Comp Neurol*. 2019;527:174–186.
87. Schwaller B, Meyer M, Schiffmann S. 'New' functions for 'old' proteins: the role of the calcium-binding proteins calbindin D-28k, calretinin and parvalbumin, in cerebellar physiology. Studies with knockout mice. *Cerebellum*. 2002;1:241–258.
88. Eisner D, Neher E, Taschenberger H, Smith G. Physiology of intracellular calcium buffering. *Physiol Rev*. 2023;103:2767–2845.
89. Wernyj RP, Mattson MP, Christakos S. Expression of calbindin-D28k in C6 glial cells stabilizes intracellular calcium levels and protects against apoptosis induced by calcium ionophore and amyloid beta-peptide. *Brain Res Mol Brain Res*. 1999;64:69–79.
90. Mattson MP, Cheng B, Baldwin SA, et al. Brain injury and tumor necrosis factors induce calbindin D-28k in astrocytes: evidence for a cytoprotective response. *J Neurosci Res*. 1995;42:357–370.
91. Zhang T, Zhu L, Madigan MC, et al. Human macular Müller cells rely more on serine biosynthesis to combat oxidative stress than those from the periphery. *Elife*. 2019;8:e43598.
92. Powner MB, Gillies MC, Tretiach M, et al. Perifoveal Müller cell depletion in a case of macular telangiectasia type 2. *Ophthalmology*. 2010;117:2407–2416.
93. Powner MB, Gillies MC, Zhu M, Vevis K, Hunyor AP, Fruttiger M. Loss of Müller's cells and photoreceptors in macular telangiectasia type 2. *Ophthalmology*. 2013;120:2344–2352.
94. Zucker CL, Bernstein PS, Schalek RL, Lichtman JW, Dowling JE. A connectomics approach to understanding a retinal disease. *Proc Natl Acad Sci U S A*. 2020;117:18780–18787.
95. Schmitz-Valckenberg S, Fleckenstein M, Helb HM, Charbel Issa P, Scholl HP, Holz FG. In vivo imaging of foveal sparing in geographic atrophy secondary to age-related macular degeneration. *Invest Ophthalmol Vis Sci*. 2009;50:3915–3921.
96. Bax NM, Valkenburg D, Lambertus S, et al. Foveal Sparing in Central Retinal Dystrophies. *Invest Ophthalmol Vis Sci*. 2019;60:3456–3467.

Investigative Ophthalmology & Visual Science